Chord-End RHS-to-RHS and CHS-to-CHS X-Connections with Rigid Cap Plates: Stress Concentration Factors

Min Sun[a,*], Kyle Tousignant[b], Ali Ziaei Nejad[a] and Sara Daneshvar[a]

[a] Department of Civil Engineering, University of Victoria, Victoria, BC, V8P 5C2, Canada

[b] Department of Civil & Resource Engineering, Dalhousie University, Halifax, NS, B3H 4R2, Canada

[*] Corresponding Author. E-mail: msun@uvic.ca

Abstract

For rectangular hollow section (RHS)-to-RHS and circular hollow section (CHS)-to-CHS connections situated near a truss/girder end, reinforcement using a chord-end cap plate is common; however, for fatigue design, formulae in current design guidelines [for calculation of stress concentration factors (SCFs)] cater to: (i) unreinforced connections, with (ii) sufficient chord continuity beyond the connection on both sides. To develop definitive design guidelines for end connections with rigid cap plates, previous full-scale connection test results have been used to validate a finite element (FE) modelling approach, and a total of 496 FE models with different chord end distance-to-width (or diameter) (e/b_0 or e/d_0), branch-to-chord width (β), branch-to-chord thickness (τ), and chord slenderness (2γ) ratios have been modelled and analyzed. Existing SCF formulae in CIDECT Design Guide 8 are shown to be inaccurate if applied to cap plate-reinforced end connections. SCF correction factors (ψ), and parametric formulae to estimate ψ based on e/b_0 (or e/d_0), β, τ and 2γ, are derived.

Keywords

Rectangular hollow sections; circular hollow sections; X-connections; end effects; stress concentration factors; fatigue design; cap plates.

[*]Corresponding Author. E-mail: msun@uvic.ca

1. Introduction

Current design standards and guidelines [1-9] for welded hollow structural section (HSS) connections tabulate limit states, associated formulae (for calculation of connection strength), and ranges of validity for formulae; however, these provisions assume a chord member (as labelled in Figs. 1a and 1d) with sufficient continuity on both sides of the connection [i.e. large end distances (*e*)]. Such connections are referred to in this paper as “regular” connections.

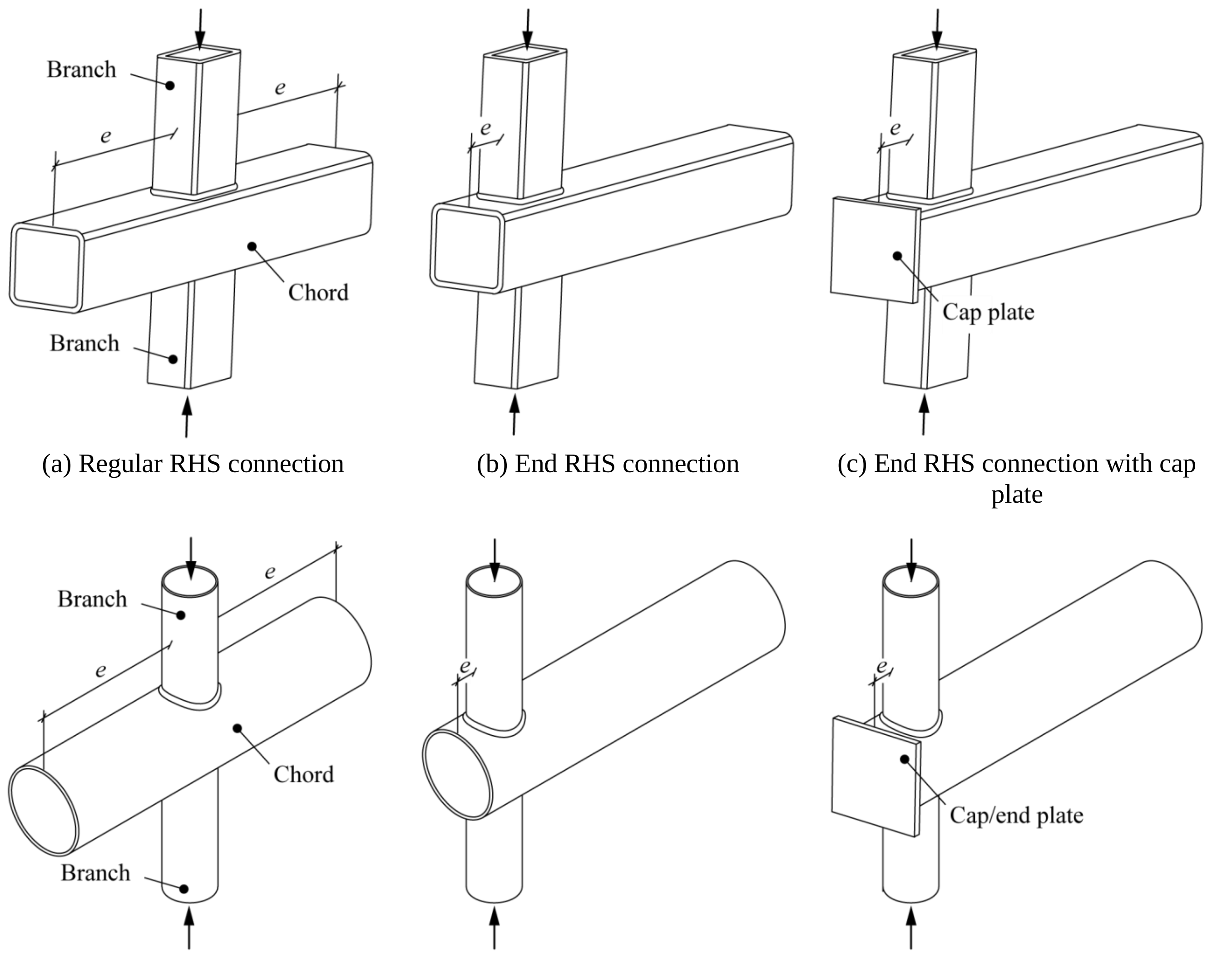

(a) Regular RHS connection

(b) End RHS connection

(c) End RHS connection with cap plate

(d) Regular CHS connection

(e) End CHS connection

(f) End CHS connection with cap plate

Fig. 1. Different types of RHS-to-RHS and CHS-to-CHS X-connections

The chord-continuity assumption inherent to current design provisions is important for connection strength calculations for several limit states, e.g. chord plastification for Rectangular Hollow Section (RHS)-to-RHS and Circular Hollow Section (CHS)-to-CHS connections, and sidewall buckling for RHS-to-RHS connections. In such cases, sufficient end distances (*e*) are required on both sides of the connection to develop the predicted failure mechanism(s) and, in turn, the full (predicted) connection strength.

For connections at the end of a truss/girder, branch(es) are usually situated near a chord end (as shown in Figs. 1b,c and 2b,c). In such cases, existing design formulae (e.g. in [1-9]) do not apply (because the chord-continuity assumption is violated). Guidance on design of these so-called "end" connections has become increasingly sought after.

To address the challenge of designing end connections, research was performed by [10-16] on directly welded RHS-to-RHS, CHS-to-CHS, and branch plate-to-CHS end connections near an open (uncapped) chord end. It was found (by [10-16]) that the static strength of the connections (and welds thereto) was reduced relative to their regular-connection counterparts. In light of this, amendments were made to EN 1993-1-8 [7] (via prEN1993-1-8 Clause 9.1.2(10) [17]), and Tables K2.1A, K3.1A and K3.2A of AISC 360-16 [5], giving requirements for so-called minimum end distances (e_{min}). A review of the above research can be found in [18,19].

When the distance from the near side of a connecting HSS branch member (or branch plate) to the open end of a chord (*e* in Fig. 1b) is less than e_{min}, AISC 360-16 [5] suggests (via the Commentary to Chapter K) a uniform reduction in predicted connection strength of 50% for RHS-to-RHS and plate-to-RHS connections; both prEN1993-1-8 Clause 9.1.2(10) [17] and AISC 360-16 [5] also suggest that providing a chord-end cap plate (Figs. 1c and 1f) is an effective design alternative. For the latter (AISC 360-16), this allows a waiver of the connection strength reduction requirement.

It should be noted that the current e_{min} requirement in AISC 360-16 [5] Table K3.2A for RHS-to-RHS truss connections ($e_{min} = b_0\sqrt{1-\beta}$ where b_0 = chord width and β = branch-to-chord width ratio) was developed based on the "chord face plastification" limit state only. Recent research [15] have shown that this limit is, in fact, unconservative, since it does not consider other limit states. [15] considered "chord side wall buckling" in addition to "chord face plastification" and proposed: (a) a new limit of $e_{min} = 0.75b_0$ for HSS connections with RHS chords and (b) a reduction in strength by 40% (instead of 50%) if $e < e_{min} = 0.75b_0$.

Prior to the above research and design standard updates, there was no definitive design guidance on truss/girder-end HSS connections under static loading. For HSS truss design and fabrication, it is a common practice to control the total number of different section sizes for cost saving, logistic and esthetic reasons. Therefore, the truss/girder-end connection and its nearby connections often have the same branch and chord sizes. However, a higher load carrying capacity is often required for end connections for load transfer to truss/girder supports. Thus, the above research and design standard updates for HSS end connections under static loading is particularly useful in this regard, as this has been a practical problem encountered by engineers [14,15]. Similarly, for an HSS truss/girder under fatigue loading, design of an end connection can often govern the branch and chord sizing for its nearby structure. Thus, it is deemed necessary in this research to extend the recent design standard updates to cover also HSS end connections under fatigue loading, as there is currently no definitive design guidance on this issue.

Research has been performed by [18,19] to address fatigue design of RHS-to-RHS and CHS-to-CHS axially loaded X-connections near an open chord end. For the connections studied, [18,19] found that existing formulae in CIDECT Design Guide 8 (DG8) [8], for the calculation of Stress Concentration Factors (SCF) (for regular connections) can be highly inaccurate. SCF correction factors (ψ), and parametric formulae to estimate ψ based on e, and non-dimensional connection parameters, were proposed. (Use of the ψ factor is discussed in Section 4.3).

As another step towards developing comprehensive fatigue design rules for chord-end RHS-to-RHS and CHS-to-CHS X-connections, this paper presents an FE parametric study to determine SCFs for such connections reinforced with cap plates. Using FE modelling approaches validated in previous investigations [18,19], this study consists of:

(1) 256 RHS connection models with variations in chord slenderness ($2\gamma = b_0/t_0$, where b_0 = chord width and t_0 = chord thickness), branch-to-chord width ratio ($\beta = b_1/b_0$, where b_1 is the branch width), branch-to-chord thickness ratio ($\tau = t_1/t_0$, where t_1 is the branch thickness] and e (on *one side* of the of the connection) = 0.1, 0.25, 1.0 and 3.0 times b_0. This terminology (for RHS-to-RHS connections) is illustrated in Fig. 2a.

(2) 240 CHS connection models with variations in chord slenderness ($2\gamma = d_0/t_0$, where d_0 = chord diameter and t_0 = chord thickness), branch-to-chord diameter ratio ($\beta = d_1/d_0$, where d_1 is the branch diameter), branch-to-chord thickness ratio ($\tau = t_1/t_0$, where t_1 is the branch thickness] and e (on *one side* of the of the connection) = 0.1, 0.25, 1.0 and 3.0 times d_0. This terminology (for CHS-to-CHS connections) is illustrated in Fig. 2b. "α" in Fig. 2b is the chord length parameter (= $2l_0/d_0$) from CIDECT DG8 [8] for consideration of chord length effect in connections symmetric about branch centerline. The details are discussed in Section 5.1.

It should be noted that $e = 3.0d_0$ (the upper value of e, above) is a conservative upper limit beyond which end-distance effects can be safely ignored [10-16].

For each connection model, SCFs at the critical locations are determined numerically and compared to the predicted values by CIDECT DG 8 [8] (for regular connections) to examine the applicability of the existing formulae. SCF correction coefficients (ψ) – and parametric formulae to estimate ψ (based on e/b_0, 2γ and β) – are then derived to increase the accuracy of the SCF predictions.

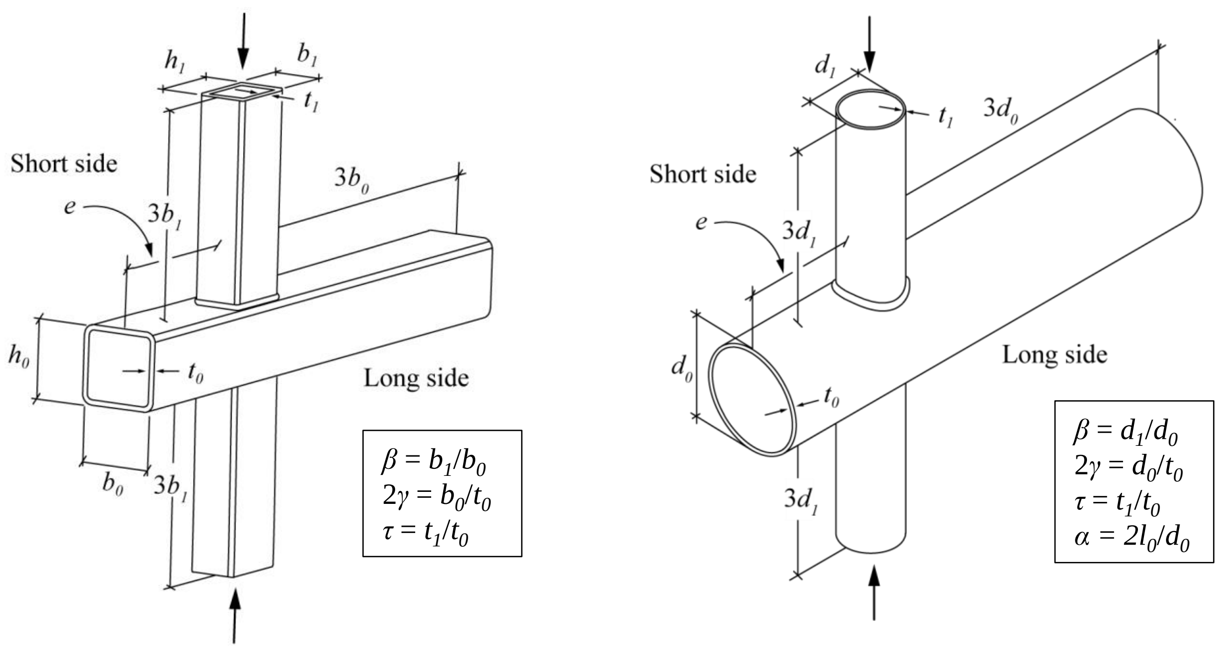

(a) RHS-to-RHS connection (b) CHS-to-CHS connection

Fig. 2. Connection terminology (end plate not shown, for clarity)

2. Relevant research on chord lengths and end conditions

In a recent experimental study on RHS-to-RHS connections with medium β-ratios [14], different yield line patterns were observed in regular connections and connections near an open chord end (see Fig. 3). Due to the reduction in the total yield line length, the static strength of an RHS-to-RHS connection near an open chord end – for the "chord face plastification" limit state – was found to be significantly smaller than that of its regular-connection counterpart. The research done by [14] broadly supports the e_{min} requirement already present in AISC 360-16 [5] Table K3.2A for RHS-to-RHS truss connections (Eq. 1), i.e.:

$$e_{\min} = b_0 \sqrt{1-\beta} \tag{1}$$

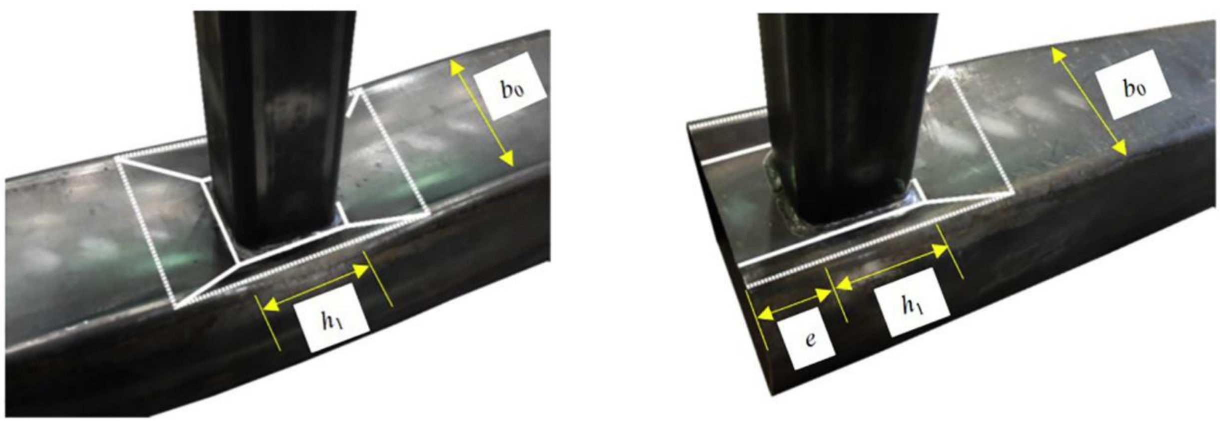

(a) Regular RHS connection (b) RHS connection near an open chord end

Fig. 3. Typical yield line patterns (adapted from [14])

The study by [14] was extended by [15], via a FE parametric study to consider both the "chord side wall buckling" and the "chord face plastification" limit states. A new limit of e_{min} = 0.75b_0 was proposed for connections with RHS chords. A 40% strength reduction (instead of 50%) was recommended when $e < e_{min}$ = 0.75b_0.

The research by [15] also found that reinforcing the open chord end with a rigid cap plate (Fig. 1c) effectively restrains the connection deformation and allows it to develop connection static strength comparable to regular connections (Fig. 1a). Therefore, for cap plate-reinforced connections, the e_{min} requirement does not apply.

Research on the effects of end distance and boundary conditions on CHS-to-CHS connections has also been performed, by [10,11]. CHS T- and X-connections covering a wide range of non-dimensional parameters (β, 2γ and τ) and chord length parameters ($\alpha = 2l_o/d_o$, where l_o = chord length) under branch axial loading were modelled. The effect of rigid chord end cap plate was also studied numerically. To prevent a significant strength reduction, the research proposed simple limits of $\alpha \geq 20$ (for chords with $2\gamma > 25$) and $\alpha \geq 12$ (for chords with $2\gamma \leq 25$). These limits were later confirmed for transverse branch plate-to-CHS T- and X-connections [14,15].

The FE parametric study by [10,11] showed that the minimum end distance requirement can be waived with the addition of a chord end cap plate, as – similar to connections with RHS chords – it largely restrained chord ovalization. In response to this research, an amendment was made to EN 1993-1-8 [7] (via prEN1993-1-8 Clause 9.1.2(10) [17]) which stipulates that:

"for joints with a chord end not connected to other members, the chord end shall be at a distance of at least $(2\gamma/10)d_0$ from the heel or toe of the closest brace, with a minimum of $2.5d_0$. For RHS chords, substitute d_0 by the largest of b_0 or h_0".

When the end-distance requirement cannot be met, the amendment suggests that the chord end shall be "welded to a cap plate with a thickness of at least $1.5t_0$, at a minimum distance of $0.5d_0(1 - \beta)$ or $0.5b_0(1 - \beta)$" from the branch toe or heel of the joint to prevent the strength reduction.

It should be noted that the minimum end distance requirement in prEN1993-1-8 Clause 9.1.2(10) [17] was developed based on research on CHS-to-CHS connections only. In this amendment to EN 1993-1-8 [7], the same requirement was transcribed to cover RHS-to-RHS connections, by replacing the CHS external diameter (d_0) with the RHS external width (b_0). However, no research evidence was available to support this transcription at the time.

Clearly, there is quite a disparity between the minimum end distance requirements in AISC 360-16 [7] and prEN1993-1-8 [19], mainly because the research by [10,11] focused on connections that were symmetrical about the branch member, while the research by [14,15] catered to end connections with reduced chord length on only one side of the connection. Nonetheless, all the above research and recent updates to design standards on connection static strength acknowledge the addition of chord-end cap plate as a solution allowing waiver of the end-distance requirement.

While research has been performed to develop design rules for HSS-(or plate-)to-HSS end connections under static loading, only limited research has been conducted on fatigue design of end connections. Recently, [18,19] performed a series of experimental and FE study to determine SCFs for directly welded RHS-to-RHS and CHS-to-CHS axially loaded X-connections at 90° near an open chord end. It was found that the existing formulae in CIDECT DG8 [8] (for regular connections) led to inaccurate SCF predictions. SCF correction factors (ψ), and parametric formulae to estimate ψ based on chord end distance and member cross-sectional dimensions (i.e. β, 2γ, τ and e/b_0) were hence derived [18,19], allowing SCFs in end connections near open chord ends to be predicted by multiplying ψ by the SCF values calculated using the existing CIDECT DG8 formulae [8].

Since it has been confirmed by [10-15] already that a chord-end cap plate can largely restrain chord deformation, and influence connection behaviour, it was deemed necessary to extend the work by [18,19] to investigate SCFs chord-end RHS-to-RHS and CHS-to-CHS X-connections with cap plates.

3. Finite Element Model Validation

3.1. Connection modelling

Commercial software programs (ANSYS and ABAQUS) [20,21] were used to conduct FE modelling and analyses of the RHS-to-RHS and CHS-to-CHS connections considered herein (see Section 1). The modelling approaches were previously validated by comparing the responses of the FE models with the experimental data of identical connections [18,19]. All modelling parameters were varied in sensitivity studies to ensure that FE models were not excessively large (computationally), but still provided convergence. The recommendations in CIDECT DG8 were followed throughout the modelling and analyses, including element selection, mesh refinement, weld details, boundary conditions and extrapolation of hot spot stress. Detailed discussions can be found in [18,19].

For modelling of RHS-to-RHS connections, four layers of solid elements (C3D20R in ABAQUS) through the branch and chord wall thicknesses were used. A “one-half model” (which was permissible due to symmetry in geometry, loading and boundary conditions along the “cut face”), as shown in Fig. 4, was used. A “symmetry boundary condition” was applied to all nodes on the “cut face”. The connection models contained fixed nodes at the bottom end of the lower branch, while the nodes on the top end of the top branch were free. The chord ends were free as well. Similarly, for modelling of CHS-to-CHS connections, four layers of solid elements (SOLID45 in ANSYS) through the branch and chord wall thicknesses were used. For regular CHS-to-CHS connections, both chord ends were pin-supported. The bottom end of the CHS lower branch was fixed, while the top end of the top CHS branch was free. For CHS-to-CHS end connections, the chord end of the shorter side was free. The selected boundary conditions are consistent with the design rules and formulae in CIDECT DG8 [8]. The selection of element type, element size and mesh pattern meet the CIDECT DG8 requirements for accurate modelling. Detailed discussions can be found in [18,19].

For practical design purpose, in the recent amendment to EN 1993-1-8 [7] via prEN1993-1-8 Clause 9.1.2(10) [17], it is recommended that when the minimum chord end distance requirement cannot be met, the end shall be welded to a cap plate with a thickness of at least $1.5t_0$. The recommended minimum cap plate thickness is determined based on [10]. Cap plate with such thickness is proven by [10] to have sufficient stiffness relative to chord sidewalls. It completely restrains local chord deformation. The cap plate has a rigid behaviour in this case.

The approach used by [10,11,16] was adopted to model the rigid chord end plates [by adding a row of stiff (E = 2×10^9 MPa) linear-elastic solid elements to the short chord end (Figs. 4b and 4d)]. A half of each connection was modelled, by taking advantage of the symmetries of geometry, loading and boundary conditions, to save computational time. Symmetry boundary conditions were applied along the cut face.

A literature survey was performed on previous research involving modelling of welds in HSS connections [22-36], and the weld modelling approach(es) was found to be consistent. A similar approach was adopted herein. It should be noted that the CIDECT DG8 approach for SCF calculation considers the uneven stress distribution around the perimeter of the welded joint, and excludes effects related to configuration of the weld (and the local condition of the weld toe).

Linear elastic material properties, including Young's modulus (E) = 200 GPa, and Poisson's ratio (ν) = 0.3, were applied to both the steel and weld materials in the FE models. Fig. 4 shows the geometry, mesh layout and boundary conditions of typical models (RHS-to-RHS and CHS-to-CHS). For each model, an axial compression force was applied in the upper branch with nodes on the end of the lower branch restrained from translation.

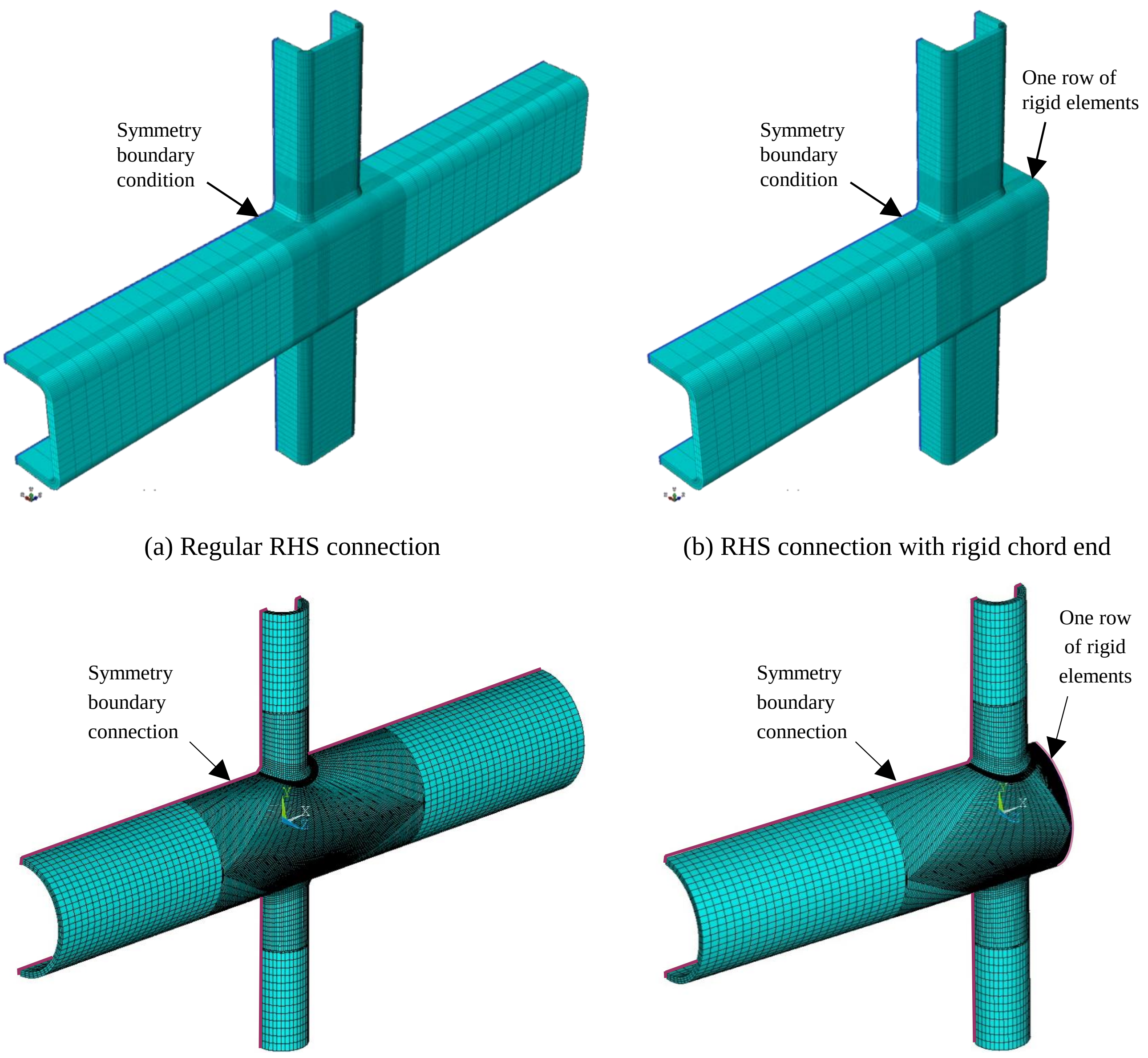

(a) Regular RHS connection

(b) RHS connection with rigid chord end

(c) Regular CHS connection

(d) CHS connection with rigid chord end

Fig. 4. Typical connection model geometry, mesh layout, and boundary conditions

In accordance with the CIDECT DG8 [8] recommendations, the welded joint location was partitioned and meshed, carefully, to allow accurate calculation of hot spot stresses within the extrapolation zones. The extrapolation zones at the critical locations are shown in Tables 1 and 2. For all FE models in this study, the hot spot stresses were calculated by using the extrapolation approach [8]. The branch nominal stress was hence calculated by dividing the applied force by the branch cross-sectional area. The SCF-values at the critical locations were then calculated by dividing the hot spot stresses by the branch nominal stress.

Table 1. Boundaries of extrapolation region for RHS-to-RHS connections

Distance from weld toe	Locations B, C and D	Locations A and E
$L_{r,min}$ *	$0.4t_0$	$0.4t_1$
$L_{r,max}$	$L_{r,min} + t_0$	$L_{r,min} + t_1$

* Minimum value for $L_{r,min}$ is 4 mm.

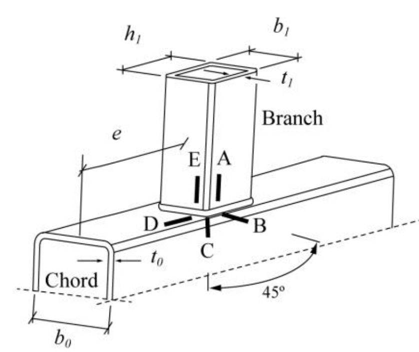

Table 2. Boundaries of extrapolation region for CHS-to-CHS connections

Distance from weld toe	Chord		Branch	
	Saddle	Crown	Saddle	Crown
$L_{r,min}$ *	$0.4t_0$	$0.4t_0$	$0.4t_1$	$0.4t_1$
$L_{r,max}$ **	$0.09r_0$	$0.4(r_0t_0r_1t_1)^{0.25}$	$0.65(r_1t_1)^{0.5}$	$0.65(r_1t_1)^{0.5}$

r_0 = external radius of CHS chord member

r_1 = internal radius of CHS branch member

* Minimum value for $L_{r,min}$ is 4 mm.

4.

** Minimum value for $L_{r,max}$ is $L_{r,min} + 0.6t_1$

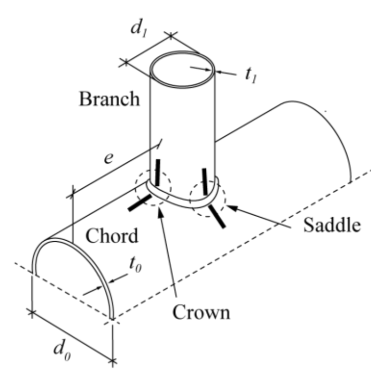

Chord-End RHS-to-RHS X-Connections with Cap Plates

In CIDECT DG8 [8], connection fatigue life is determined by using hot spot stress vs. fatigue life (S-N) curves. The hot spot stresses are calculated by multiplying the member nominal stresses by the SCFs at the critical locations. In this section, the SCF data from the parametric study for RHS-to-RHS connections are compared to the predicted values calculated using the existing SCF formulae in CIDECT DG8 [8]. The relationships among the SCF-values, the member cross-sectional dimensions, and the chord end distances are explored. Revised formulae are developed for calculation of SCFs in chord-end RHS-to-RHS X-connections with cap plates.

4.1. CIDECT Design Guide 8 Formulae

For RHS connections, CIDECT DG8 [8] considers five hot spot stress locations (locations A to E in Table 1). The CIDECT DG8 SCF formulae for regular RHS-to-RHS axially loaded T- and X-connections at these locations are as follows:

- For the chord:

$$SCF_B = \left(0.143 - 0.204\beta + 0.064\beta^2\right)\left(2\gamma\right)^{\left(1.377+1.715\beta-1.103\beta^2\right)} \tau^{0.75} \tag{2}$$

$$SCF_C = \left(0.077 - 0.129\beta + 0.061\beta^2 - 0.0006\gamma\right)\left(2\gamma\right)^{\left(1.565+1.874\beta-1.028\beta^2\right)} \tau^{0.75} \tag{3}$$

$$SCF_D = \left(0.208 - 0.387\beta + 0.209\beta^2\right)\left(2\gamma\right)^{\left(0.925+2.389\beta-1.881\beta^2\right)} \tau^{0.75} \tag{4}$$

where SCF_B, SCF_C, and SCF_D = chord SCFs at hot spot B, C, and D, respectively.

- For the branch(es):

$$SCF_A = SCF_E = \left(0.013 + 0.693\beta - 0.278\beta^2\right)\left(2\gamma\right)^{\left(0.790+1.898\beta-2.109\beta^2\right)} \tag{5}$$

where $SCF_A = SCF_E$ = branch SCF at hot spots A and E, respectively.

Eqs. (2)-(5) are valid within the following range of validity: $0.35 \le \beta \le 1.0$, $12.5 \le 2\gamma \le 25$, $0.25 \le \tau \le 1.0$.

For connections with fillet welds, SCF_A and SCF_E are multiplied by 1.4, and for X-connections with $\beta = 1.0$, SCF_C is multiplied by 0.65 and SCF_D is multiplied by 0.50. A minimum SCF-value of 2.0 is recommended by CIDECT DG8 [8] at all locations.

4.2. Parametric Study

The FE parametric study for RHS-to-RHS X-connections consisted of 64 regular connection models and 192 cap plate-reinforced end connection models. A constant RHS chord member external width and height ($b_0 = h_0$) of 200 mm, and a wide ranges of non-dimensional parameters (β = 0.35, 0.5, 0.65, and 0.8; 2γ = 12.5, 16, 20 and 25; and τ = 0.25, 0.5, 0.75, and 1.0) were applied. The chord thickness (t_0) and branch cross-sectional dimensions ($b_1 = h_1$ and t_1) were hence determined based on the selected non-dimensional parameters. The end distance (e) was varied between $0.1b_0$, $0.5b_0$, $1.0b_0$ and $3.0b_0$, with $3.0b_0$ representing a conservative upper, beyond which "end effects" can be safely ignored [10-16]. The 64 "control models", with $e = 3b_0$ on both sides, served as the basis for the parametric study. For the control models, the SCF formulae in CIDECT DG8 [8] [i.e. Eqs. (2)-(5)] are valid, in theory.

For the control models, the numerically obtained SCF-values on the two sides of the connections are the same due to symmetry. For the end connection models (i.e. those with $e < 3.0b_0$), the SCFs were obtained at the critical locations (Locations A to E, in Table 1) on both the long chord side and the cap plate-reinforced (short) chord side of the connection (see Fig. 2a). The values on the two sides were then compared – to identify the governing side. Representative data is shown in Fig. 5. According to the comparison using <u>all</u> parametric study results, it was found, for RHS-to-RHS end connections, that the long chord side is always the governing side.

As shown by the representative data in Fig. 5 (on the following page), the cap plate-reinforced short chord side has smaller SCFs values at all hot-spot locations. It is pointed out in CIDECT DG8 [8] that, for regular RHS-to-RHS X-connections under branch axial loading, the lower the 2γ ratio, the lower is the SCF, where $2\gamma = b_0 / t_0$ is an indicator of connection flexibility. In other words, for regular RHS-to-RHS connections, the SCFs at all hot-spot locations increase as the connection flexibility increases. This is consistent with the trend shown in Fig. 5. For the cap plate-reinforced short chord side, the connection deformation is largely restrained by the cap plate (i.e. the long chord side is more flexible). In the following discussion, only the SCF-values from the governing sides are used for formulae development.

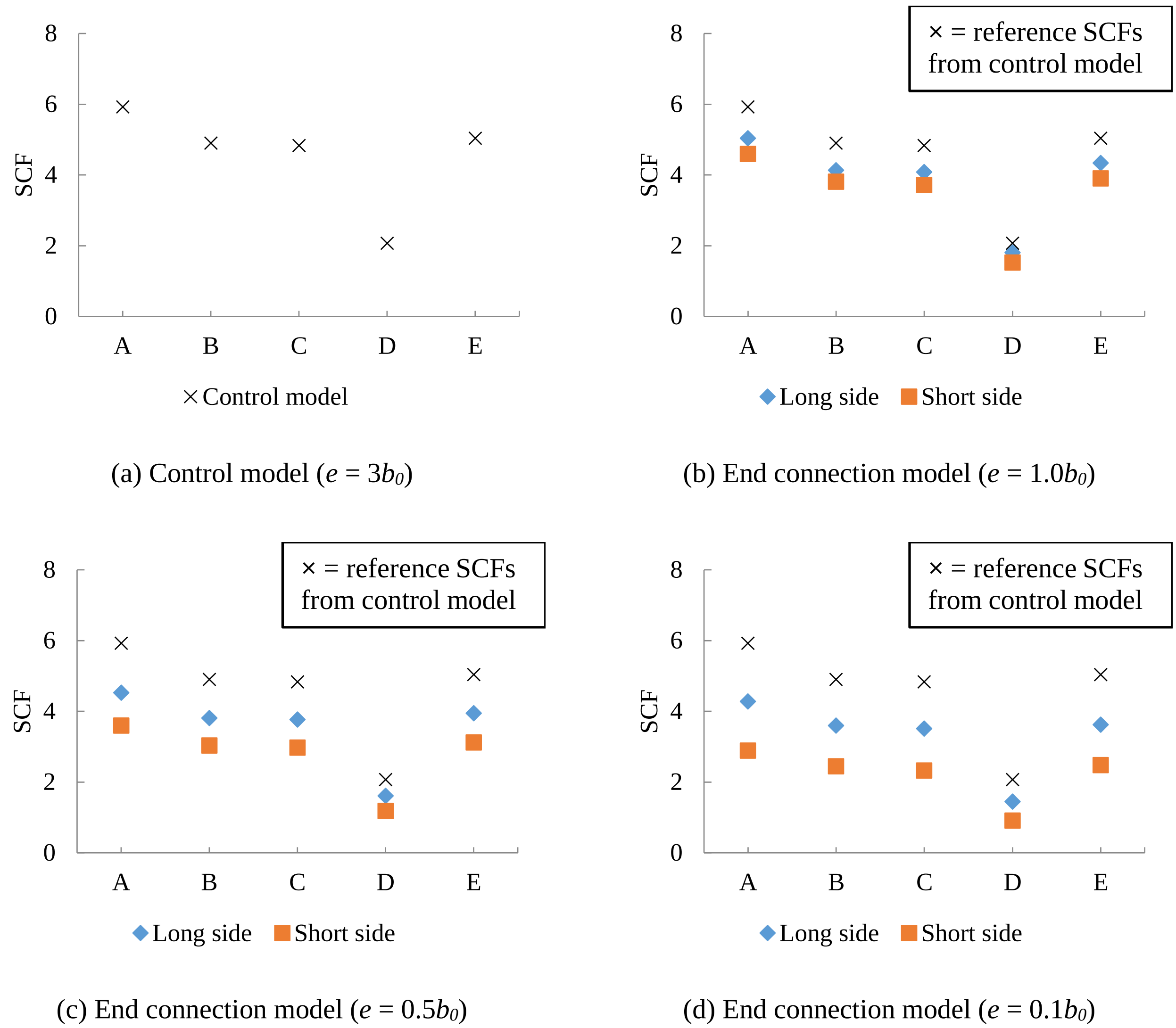

(a) Control model ($e = 3b_0$)

(b) End connection model ($e = 1.0b_0$)

(c) End connection model ($e = 0.5b_0$)

(d) End connection model ($e = 0.1b_0$)

Fig. 5. SCFs for RHS-to-RHS connection models with $\beta = 0.65$, $2\gamma = 12.5$ and $\tau = 0.5$

The SCF-values from the end connection models (with different end distances) were also compared to the predictions using the existing CIDECT DG8 [8] formulae for regular connections [i.e. Eq. (2)-(5)]. According to the representative comparisons shown in Fig. 6, the application of existing formulae can be excessively conservative. Therefore, modified formulae catering specifically to chord-end RHS-to-RHS X-connections with cap plates are deemed necessary.

The relationships among the SCF-values, the connection nondimensional parameters, the chord end distance and chord end cap plate were further explored using the parametric study results by calculating ψ equal to the ratios of SCFs in the cap plate-reinforced end-connection models ($SCF_{end\ connection}$) to those in the corresponding control models ($SCF_{control\ model}$). Representative plots of ψ (= $SCF_{end\ connection}$/ $SCF_{control\ model}$) vs. e/b_0 at the five hot-spot locations (identified in Table 1) are shown in Figs. 7-9, where e/b_0 is the chord end distance-over-chord width ratio. The following observations can be made (for all hot-spot locations):

i) ψ in general decreases as e/d_0 decreases.

ii) For different e/d_0, ψ increases as β decreases, or as 2γ increases.

iii) ψ does not change significantly for different τ.

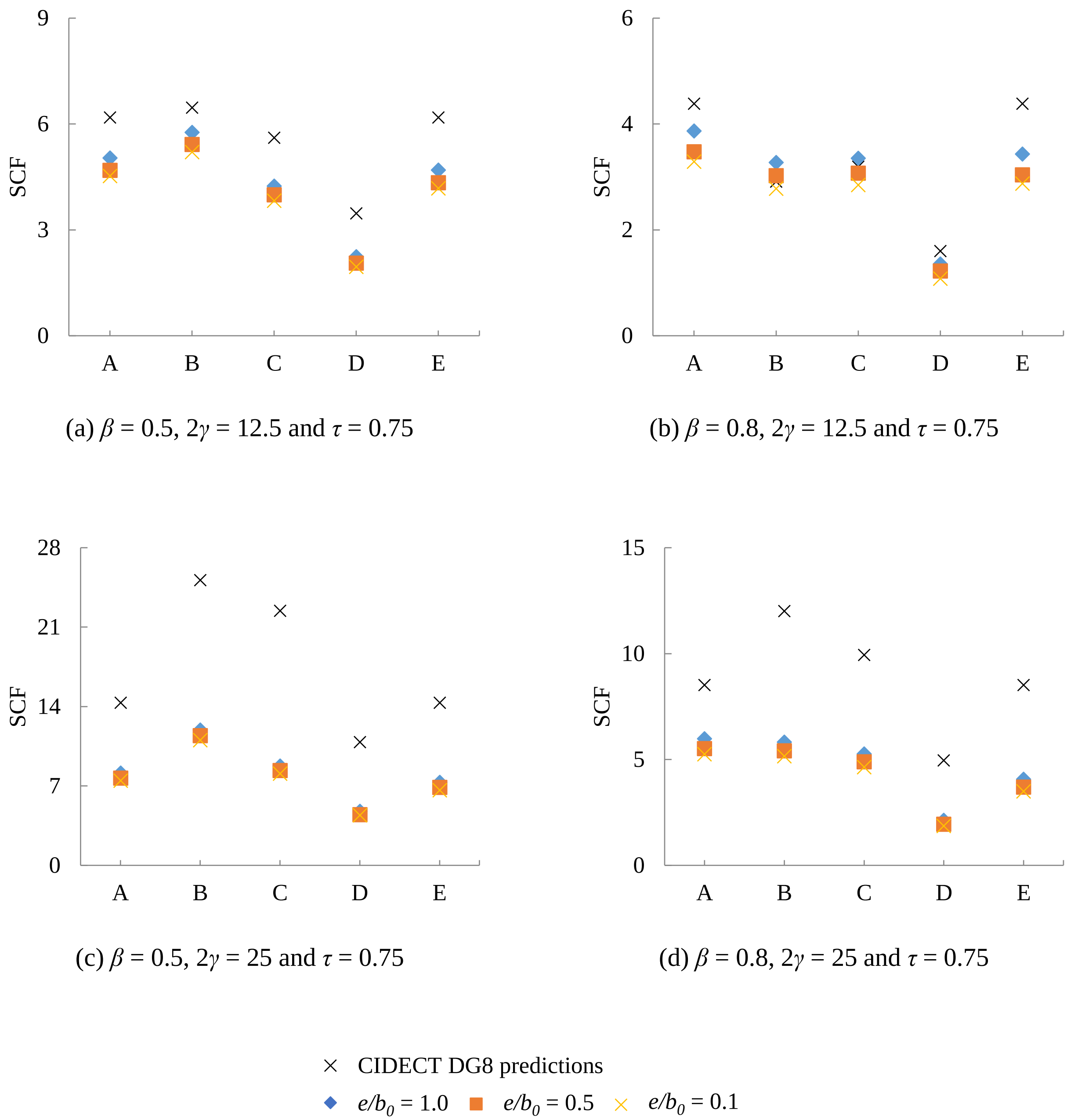

Fig. 6. Comparison of FE results for RHS-to-RHS end connections with predictions by CIDECT DG8 [8]

280

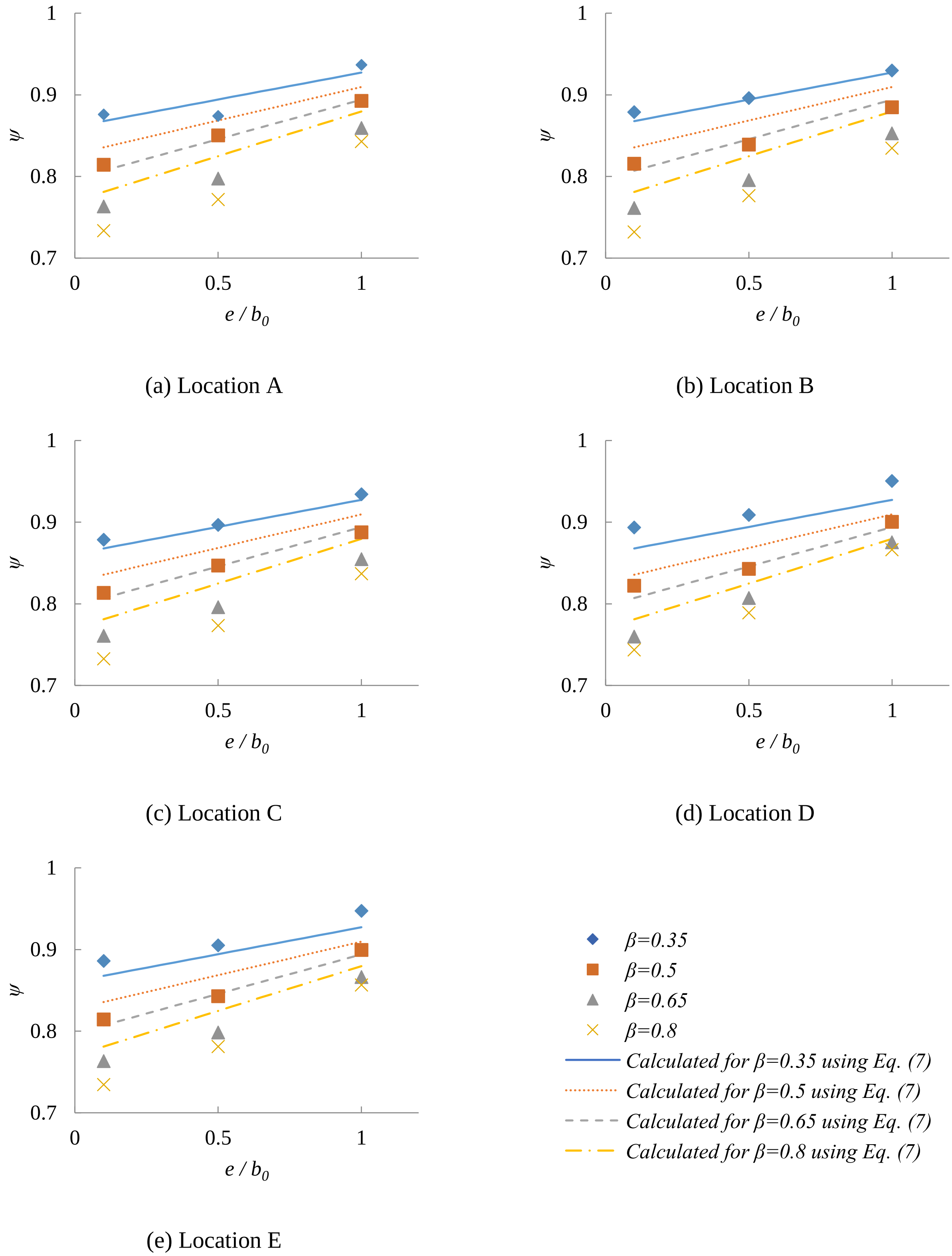

Fig. 7. Effects of e/b_0 and β on SCFs in RHS-to-RHS end connections (2γ=20 and τ=0.75)

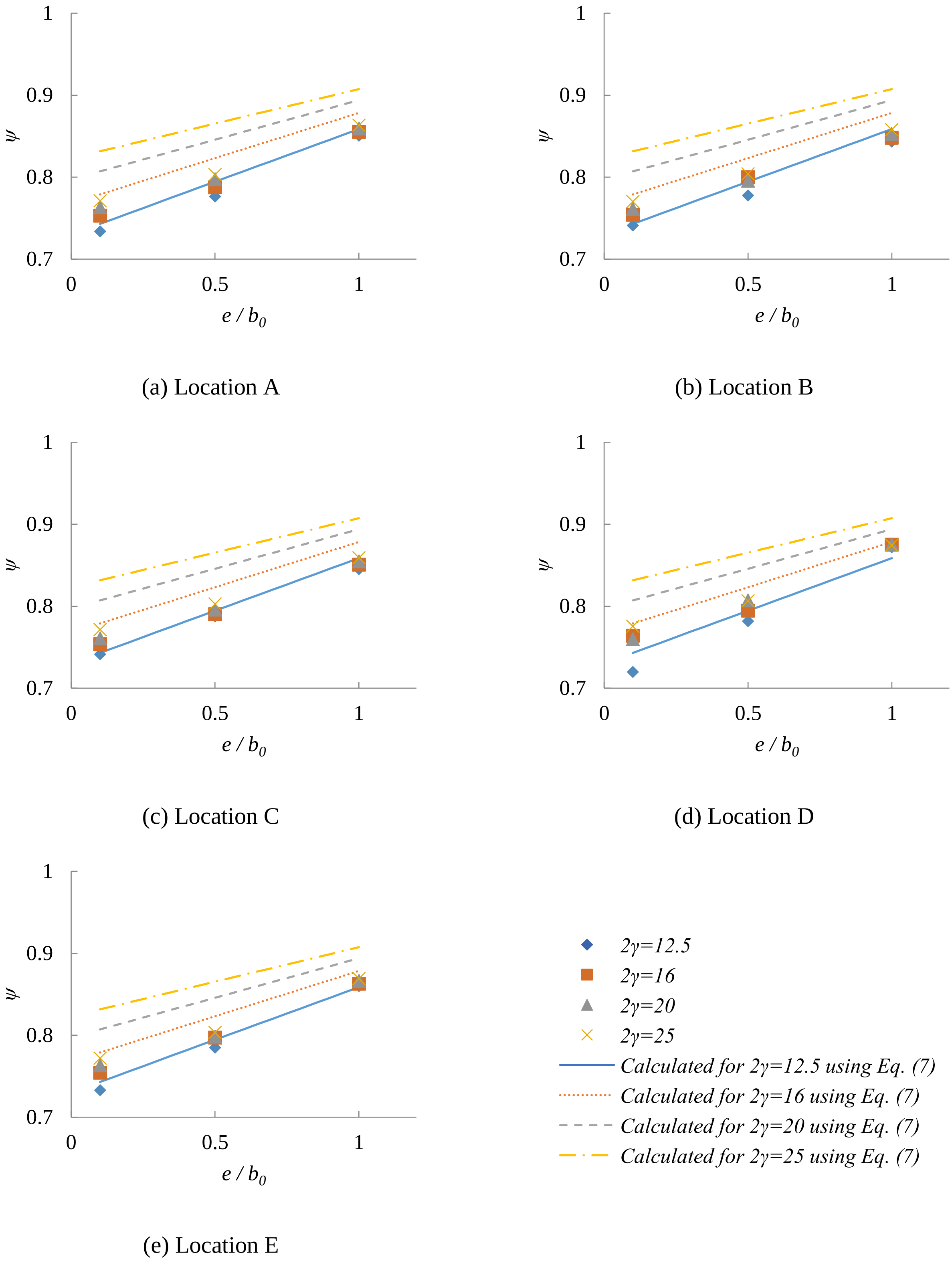

Fig. 8. Effects of e/b_0 and 2γ on SCFs in RHS-to-RHS end connections (β=0.65 and τ=0.75)

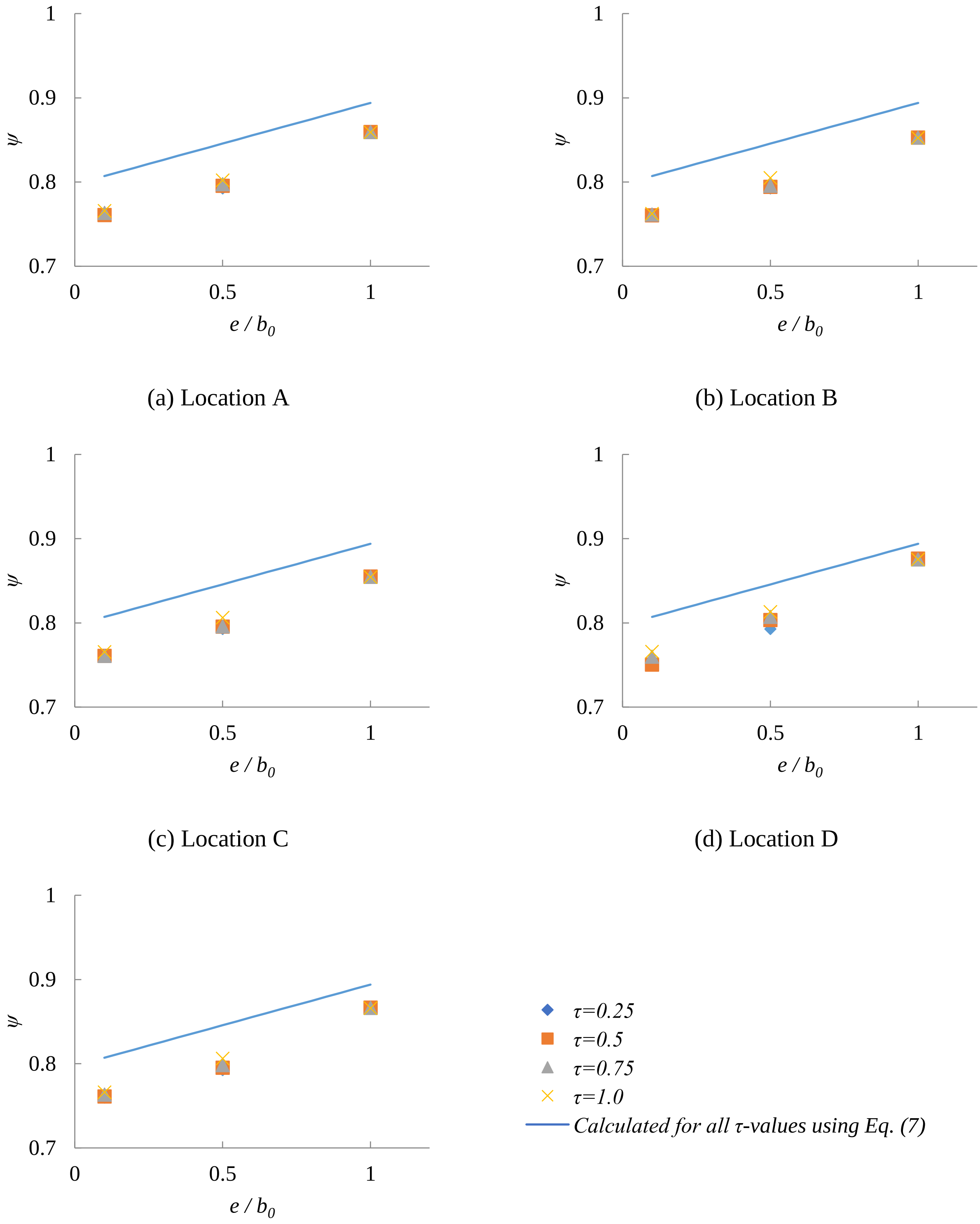

(a) Location A

(b) Location B

(c) Location C

(d) Location D

(e) Location E

Fig. 9. Effects of e/b_0 and τ on SCFs in RHS-to-RHS end connections (β=0.65 and 2γ=20)

4.3. Proposed Formulae

According to the parametric study, the SCFs in regular RHS X-connections and chord-end RHS X-connections with cap plates can differ considerably. For the latter, predictions using the existing CIDECT DG 8 [8] SCF formulae are inaccurate [because the change of chord end distance and boundary conditions (i.e. effects of chord end distance and cap plate) were not considered in their development].

As shown by Eq. 6, the ψ-factors presented above can be used in conjunction with existing CIDECT DG8 SCF formulae [i.e. by multiplying the result of Eqs. (2)-(5) by ψ] to determine the SCFs in axially loaded chord-end RHS X-connections with cap plates; i.e.:

$$SCF_{end,i} = SCF_i \cdot \psi \tag{6}$$

where SCF_i = SCF at hot spot i in a regular HSS-to-HSS X-connection [calculated using Eqs. (2)-(5)]; ψ = correction factor; $SCF_{end,i}$ = SCF at hot spot i in a chord-end HSS-to-HSS X-connection with cap plate.

As discussed in Section 4.2, in the parametric study, SCFs were obtained from the cap plate-reinforced end connection models (with $e = 0.1b_0$, $0.5b_0$, $1.0b_0$), and from the control connections (with $e = 3b_0$). The correction factors (ψ) were obtained by dividing the former by the latter.

The parametric study shows that, for each chord-end RHS X-connection with cap plate, the ψ-values for each hot spot location (i.e. A-E) are nearly constant for a given set of non-dimensional parameters. For example, for any given e/b_0 in Figs. 7, 8 and 9, the ψ-values for hot spot locations A-E only vary slightly. This is because all locations are adjacent to the branch corner at the welded joint. It was thus deemed appropriate to use a single formula to estimate the maximum of the five ψ-values (from locations A-E) in a chord-end RHS X-connection with cap plate for determination of SCFs according to Eq. (6).

As discussed in Section 4.2, for all hot spot locations, ψ changes as e/d_0, β and 2γ change. ψ does not vary significantly for different τ. An extensive evaluation of different types of formulae was conduct, followed by a non-linear least-squares regression analysis. The resulting approximate "best-fit" equation is given by Eq. (7):

$$\psi = 1 - 0.78\left(2.10 - e/b_0\right) \Big/ \left(2\gamma/\beta\right)^{0.61} \tag{7}$$

Figs. 7-9 show sample comparisons between: (i) ψ-values calculated using Eq. (7) and (ii) ψ-values obtained by dividing $SCF_{end\ connection}$ by $SCF_{control\ model}$ (based on the parametric study results). Table 3 includes the key statistics from comparisons based on the complete parametric study (i.e. 64 regular connection models and 192 end connection models). As shown in Figs. 7-9 and Table 3, Eq. (7) is reasonably accurate over the range of parameters considered. For consistency with CIDECT DG 8 [8], a minimum SCF-value of 2.0 is still recommended.

Table 3. Mean values and COVs of FE-to-predicted ψ based on Eq. (7) for 192 RHS-to-RHS cap plate-reinforced end X-connection models

Location	Mean	COV
A	0.98	0.03
B	0.98	0.03
C	0.98	0.03
D	0.98	0.04
E	0.98	0.03

5. Chord-End CHS-to-CHS X-Connections with Cap Plates

In this section, the SCF data from the parametric study for CHS-to-CHS connections are compared to the predicted values calculated using existing SCF formulae in CIDECT DG8 [8]. The relationships among the SCF-values, the member cross-sectional dimensions and the chord end distances are explored. A modified approach is developed for calculation of SCFs in chord-end CHS-to-CHS X-connections with cap plates.

5.1. CIDECT Design Guide 8 Formulae

For a CHS-to-CHS connections with a 90° branch-to-chord angle, CIDECT DG8 [8] considers four hot spot stress locations (the chord saddle, chord crown, branch saddle and branch crown, as shown in Table 2). The CIDECT formulae for regular CHS-to-CHS axially loaded X-connections for calculation of SCFs at these locations are as follows:

- For the chord:

$$SCF_{ch\_saddle,ax} = X_1 \cdot F_2 \tag{8}$$

$$SCF_{ch\_crown,ax} = X_2 \tag{9}$$

where $SCF_{ch\_saddle,ax}$ = chord SCF at the saddle point; $SCF_{ch\_crown,ax}$ = chord SCF at the crown point; and F_2 = reduction factor to account for "chord length effect" [19].

- For the branch(es):

$$SCF_{b\_saddle,ax} = X_3 \cdot F_2 \tag{10}$$

$$SCF_{b\_crown,ax} = X_4 \tag{11}$$

where $SCF_{b\_saddle,ax}$ = branch SCF at the saddle point; and $SCF_{b\_crown,ax}$ = branch SCF at the crown point.

The parameters X_1, X_2, X_3, X_4 and F_2 are given as:

$$X_1 = 3.87 \cdot \gamma \cdot \tau \cdot \beta \left[1.10 - \beta^{1.8}\right] \cdot \left(\sin\theta\right)^{1.7} \tag{12}$$

$$X_2 = \gamma^{0.2} \cdot \tau \left[2.65 + 5 \cdot \left(\beta - 0.65\right)^2\right] - 3 \cdot \tau \cdot \beta \cdot \sin\theta \tag{13}$$

$$X_3 = 1 + 1.9 \cdot \gamma \cdot \tau^{0.5} \cdot \beta^{0.9} \cdot \left(1.09 - \beta^{1.7}\right) \cdot \sin^{2.5}\theta \tag{14}$$

$$X_4 = 3 + \gamma^{1.2} \cdot \left[0.12 \cdot \exp\left(-4 \cdot \beta\right) + 0.011 \cdot \beta^2 - 0.045\right] \tag{15}$$

If $\alpha \geq 12$: $$F_2 = 1.0 \tag{16}$$

If $\alpha < 12$: $$F_2 = 1 - \left(1.43 \cdot \beta - 0.97 \cdot \beta^2 - 0.03\right) \cdot \gamma^{0.04} \cdot \exp\left(-0.71 \cdot \gamma^{-1.38} \cdot \alpha^{2.5}\right) \tag{17}$$

where θ = acute angle between the branch and chord (in degrees).

The above equations [Eqs. (8)-(17)] are valid within the following range of validity: $0.2 \leq \beta \leq 1.0$, $15 \leq 2\gamma \leq 64$, $0.2 \leq \tau \leq 1.0$, $4 \leq \alpha \leq 40$, and $30° \leq \theta \leq 90°$. As for RHS-to-RHS connections, a minimum SCF-value of 2.0 is still recommended [8].

It can be seen from Eqs. (16) and (17) the CIDECT DG8 [8] acknowledges end effects on SCFs in CHS-to-CHS connections. Detailed discussion on the background of these formulae can be found in [18,19]. The correction factor (F_2) is, for selected connection geometries, plotted against α over its range of validity ($4 \leq \alpha \leq 12$), and beyond its range of validity ($\alpha < 4$) to illustrate the predicted end effect in Fig. 10.

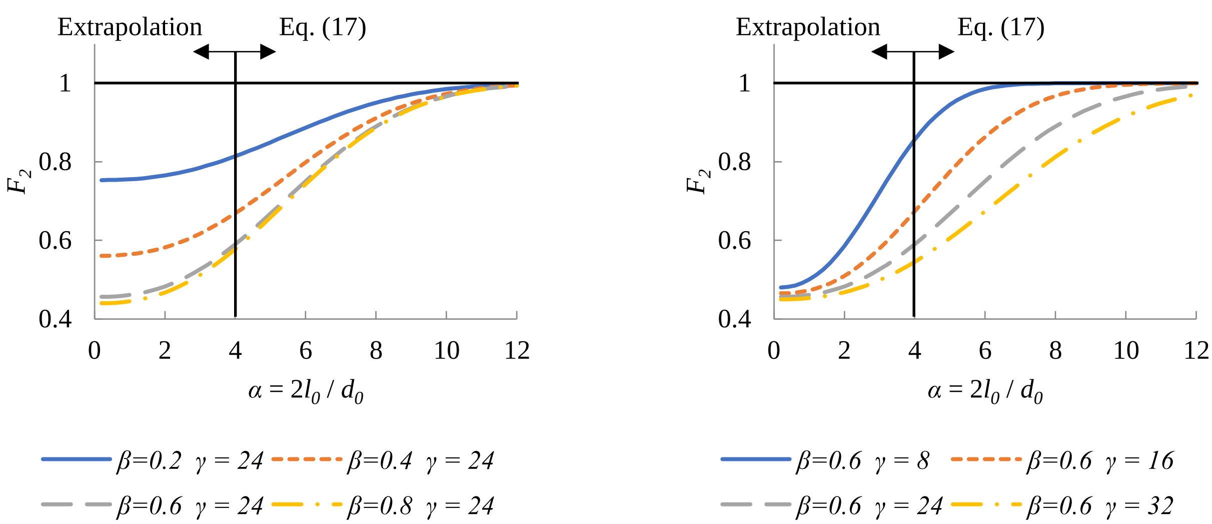

(a) Effect of β (γ = 24) (b) Effect of γ (β = 0.6)

Fig. 10. Effects of chord length and non-dimensional parameters on SCFs in CHS-to-CHS axially loaded X-connections based on CIDECT DG 8 [8] and extrapolation

5.2. Parametric Study

The FE parametric study for CHS-to-CHS X-connections consisted of 60 regular connection models and 180 cap plate-reinforced end connection models. A constant CHS chord member external diameter (d_0) of 300 mm was applied, with chord member thickness ranging from 2.4 to 15.0 mm, covering a wide range of non-dimensional parameters (β = 0.30, 0.45, 0.60, and 0.75; 2γ = 20, 35, 50 and 65; and τ = 0.4, 0.6, 0.8, and 1.0). The branch member external diameter (d_1) and thickness (t_1) were determined based on the selected non-dimensional parameters. The end distance (e) was varied between $0.1b_0$, $0.5b_0$, $1.0b_0$ and $3.0b_0$, with $3.0b_0$ representing a conservative upper limit for which "end effects" could be safely ignored [10-16].

For the 60 regular connection models (i.e. control models), the numerically obtained SCF-values on the two sides of the connections are the same due to geometrical symmetry. For the 180 end connection models, the SCFs were obtained at the hot-spot locations shown in Table 2, including: (a) chord saddle and branch saddle in Table 2; and (b) chord crown and branch saddle on both the long chord side and the cap plate-reinforced short chord side of the connection. The values on the two sides were compared to identify the governing side.

According to the comparison using parametric study results from the 180 CHS-to-CHS end connection models, it was found that for the chord crown and branch crown locations of the end connections, the cap plate-reinforced short chord side is always the governing side. As shown by the representative data in Fig. 11, the cap plate-reinforced short chord side has larger SCF-values at the critical locations. It is pointed out in CIDECT DG8 [8] that for regular CHS-to-CHS X-connections under branch axial loading, for the crown location, the lower the 2γ ratio, the higher is the SCF, where $2\gamma = b_0 / t_0$ is an indicator of connection flexibility. In other words, for the crown locations in regular CHS-to-CHS connections, the SCFs increase as the connection flexibility decreases. This is consistent with the trend shown in Fig. 11. For the cap plate-reinforced short chord side, the connection deformation is largely restrained by the cap plate (i.e. the long chord side is more flexible). Therefore, for all 180 CHS-to-CHS end connection models in the parametric study, the cap plate-reinforced short sides are the governing sides. In the following discussion, only the SCF-values from the governing sides are used for formulae development.

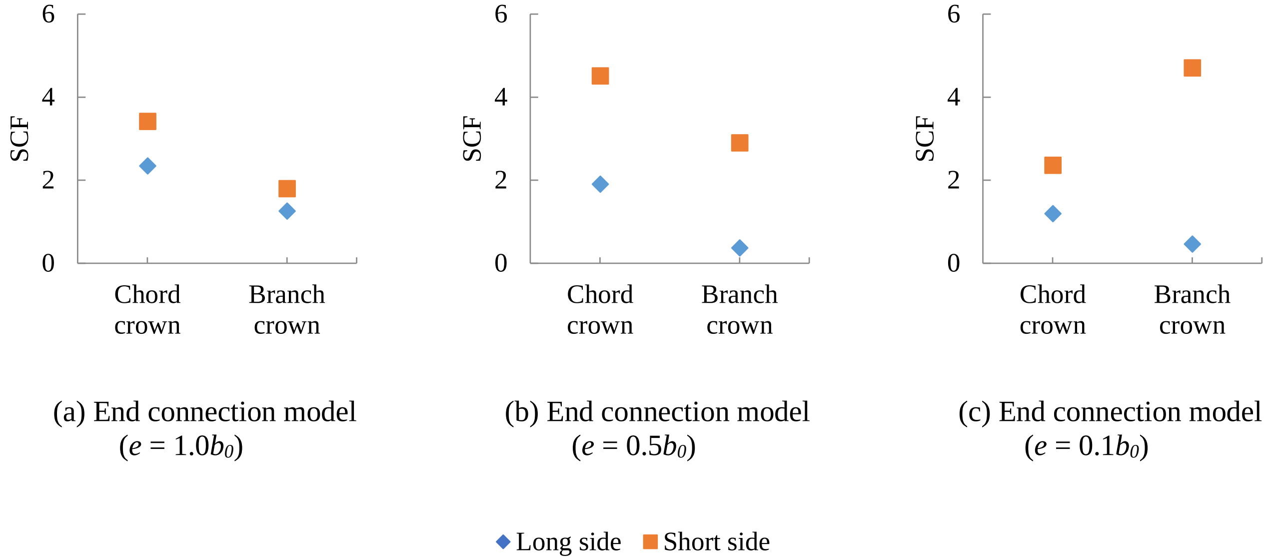

(a) End connection model (e = 1.0b_0)

(b) End connection model (e = 0.5b_0)

(c) End connection model (e = 0.1b_0)

Fig. 11. SCFs for CHS-to-CHS connection models with β = 0.45, 2γ = 20 and τ = 0.6

The "F_2" factor (Eq. 17) adopted by CIDECT DG8 [8] for consideration of chord length effect in symmetric connections is also evaluated using the FE results from the end connection models (with different end distances). Representative comparisons are shown in Figs. 12 and 13, where the ratios of SCFs in the end-connection models ($SCF_{end\ connection}$) to those in the control models ($SCF_{control\ model}$) – herein denoted as ψ – are plotted. The ratio ψ = $SCF_{end\ connection}$/ $SCF_{control\ model}$ is akin to the factor F_2 in Eq. 17. Using the α value corresponding to the end distance of the "short side", the actual and extrapolated values of F_2 for the chord and branch saddle locations are calculated using Eq. 17, and plotted in Figs. 12 and 13. The following observations can be made:

(1) The SCFs at the chord crown and branch crown locations of chord-end CHS X-connections with cap plates can be significantly larger than those in the regular connection counterparts, since the corresponding ψ-values are larger than unity. Currently, CIDECT DG8 [8] does not have a dedicated formula for consideration of the effects of chord-end cap plate on the SCFs at the chord crown and branch crown locations. For the chord saddle locations, the ψ-values are significantly smaller than the F_2-values calculated by Eq. 17. On the then hand, for the branch saddle locations, the ψ-values and the F_2-values are similar.

(2) In all cases, the ψ-values approach unity when the e/d_0-value approaches 3.0 (i.e. the effects of chord length and boundary condition become negligible), which is consistent with the findings in previous research [10-16].

In all, the existing CIDECT DG8 formula for consideration of chord length effects (i.e. Eq. 17) cannot be directly applied to chord-end CHS-to-CHS X-connections with cap plates.

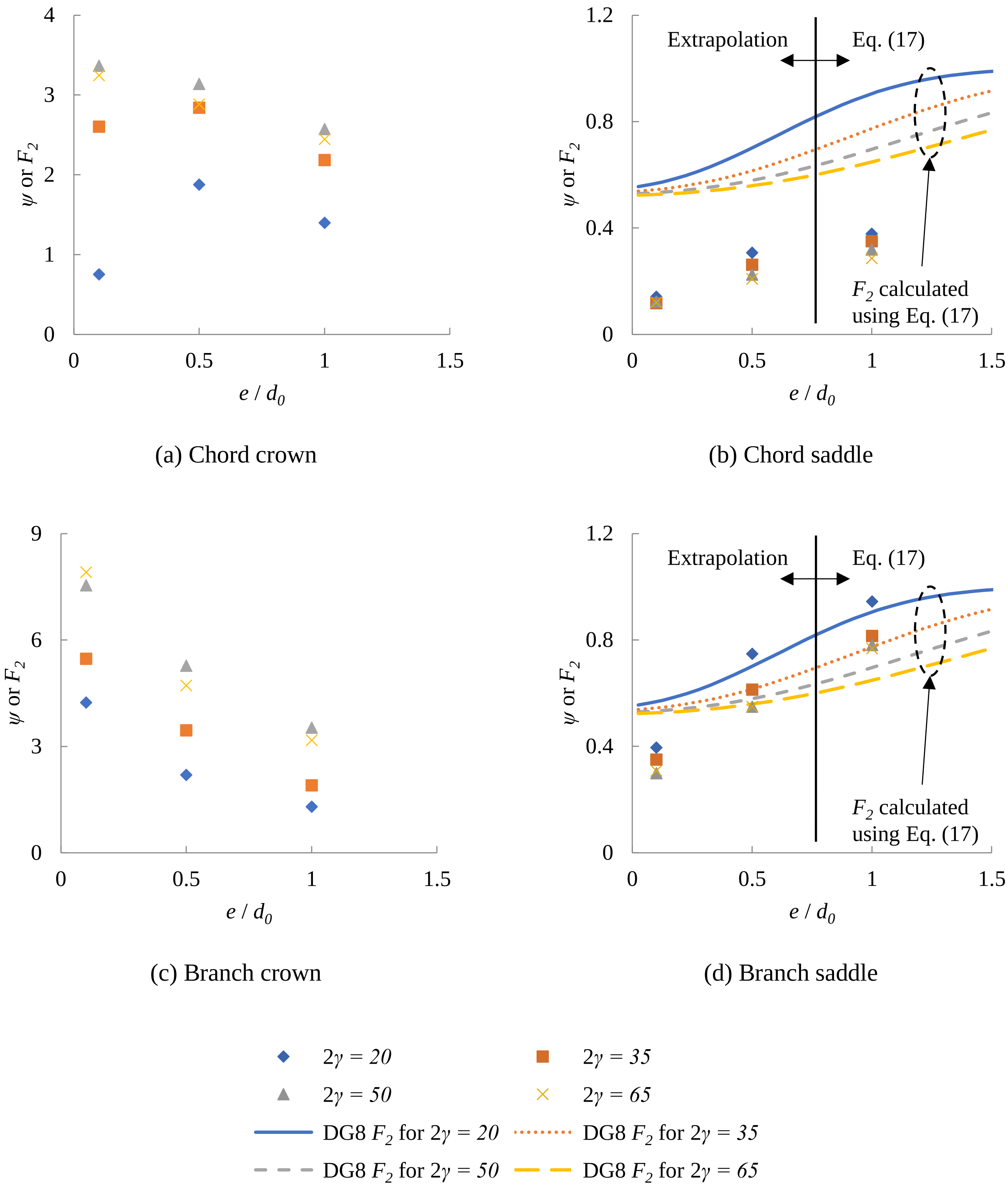

Fig. 12. SCFs for CHS-to-CHS connection models in Table 4 with $\beta = 0.45$

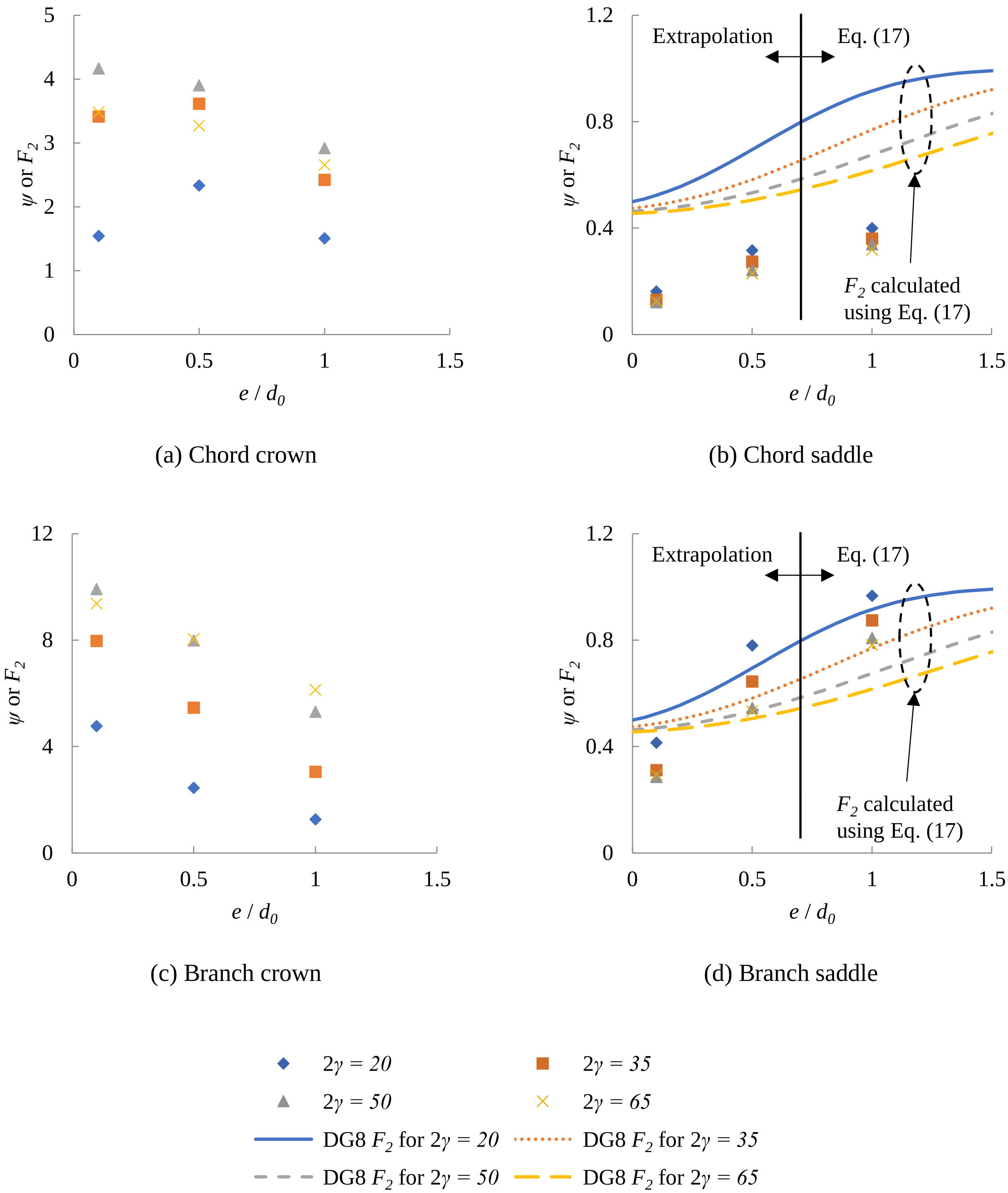

Fig. 13. SCFs for CHS-to-CHS connection models in Table 4 with $\beta = 0.60$

The relationships among the SCF-values, the connection nondimensional parameters, the chord end distance and chord end cap plate are further explored, using the parametric study results. Representative results of ψ (= $SCF_{end\ connection}$/ $SCF_{control\ model}$) vs. e/d_0 at the four hot-spot locations (shown in Table 2) are shown in Figs. 14-16, where e/b_0 is the chord end distance-over-chord diameter ratio. The following observations can be made:

(1) For the chord saddle and branch saddle locations, ψ increases as e/d_0 increases. On the other hand, for the chord crown and branch crown locations, ψ in many cases increases as e/d_0 decreases. For the chord crown location, the relationships between ψ and e/d_0 can be nonlinear.

(2) For the chord crown and branch crown locations, for different e/d_0, ψ in general increases as 2γ, τ and β increase.

(3) For the chord saddle and branch saddle locations, for different e/d_0, ψ in general increases as 2γ decreases, or as β increases.

(4) For the chord saddle and branch saddle locations, for different e/d_0, ψ does not change significantly for different τ.

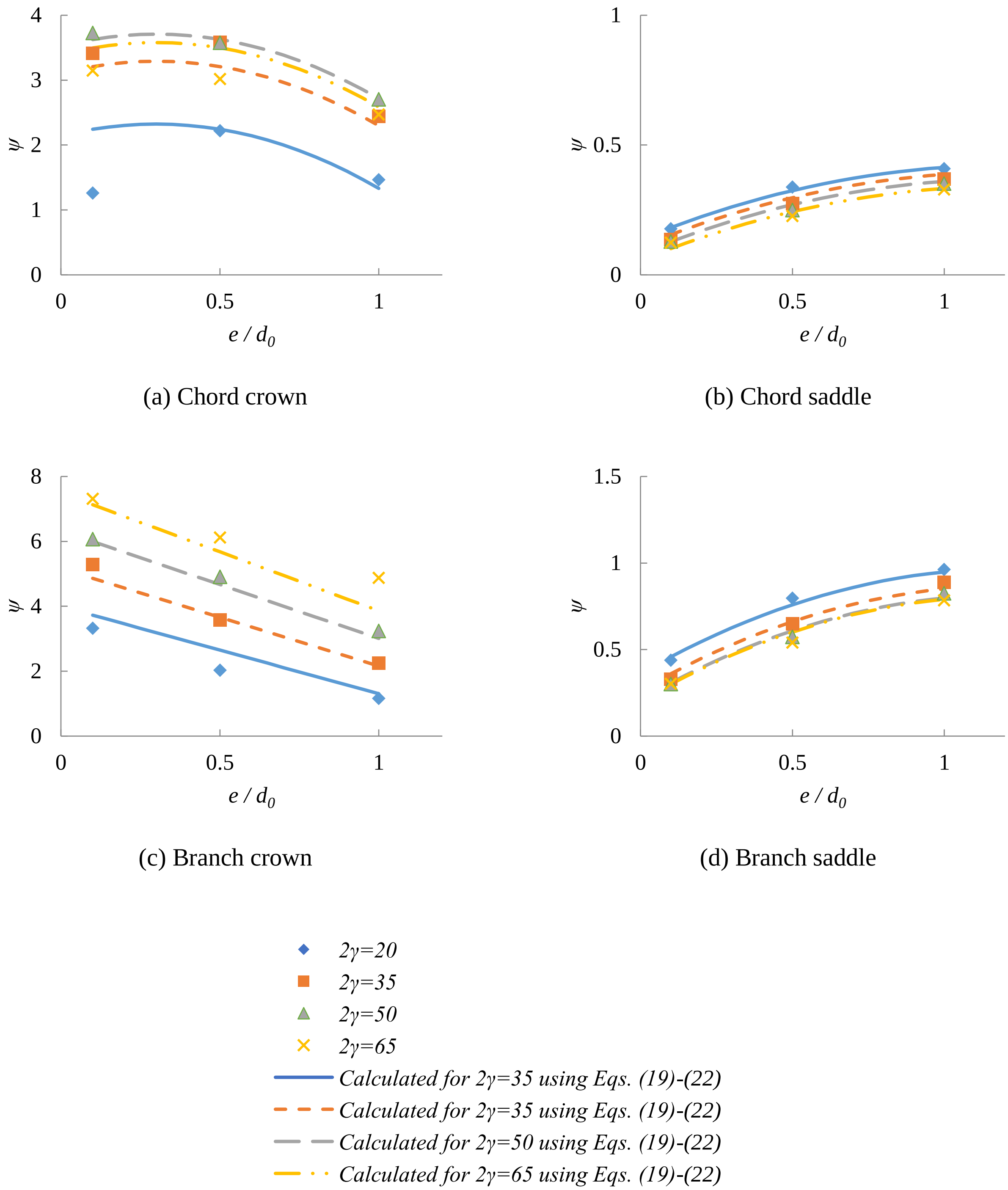

Fig. 14. Effects of e/d_0 and 2γ on SCFs in connections (β = 0.6 and τ = 0.6)

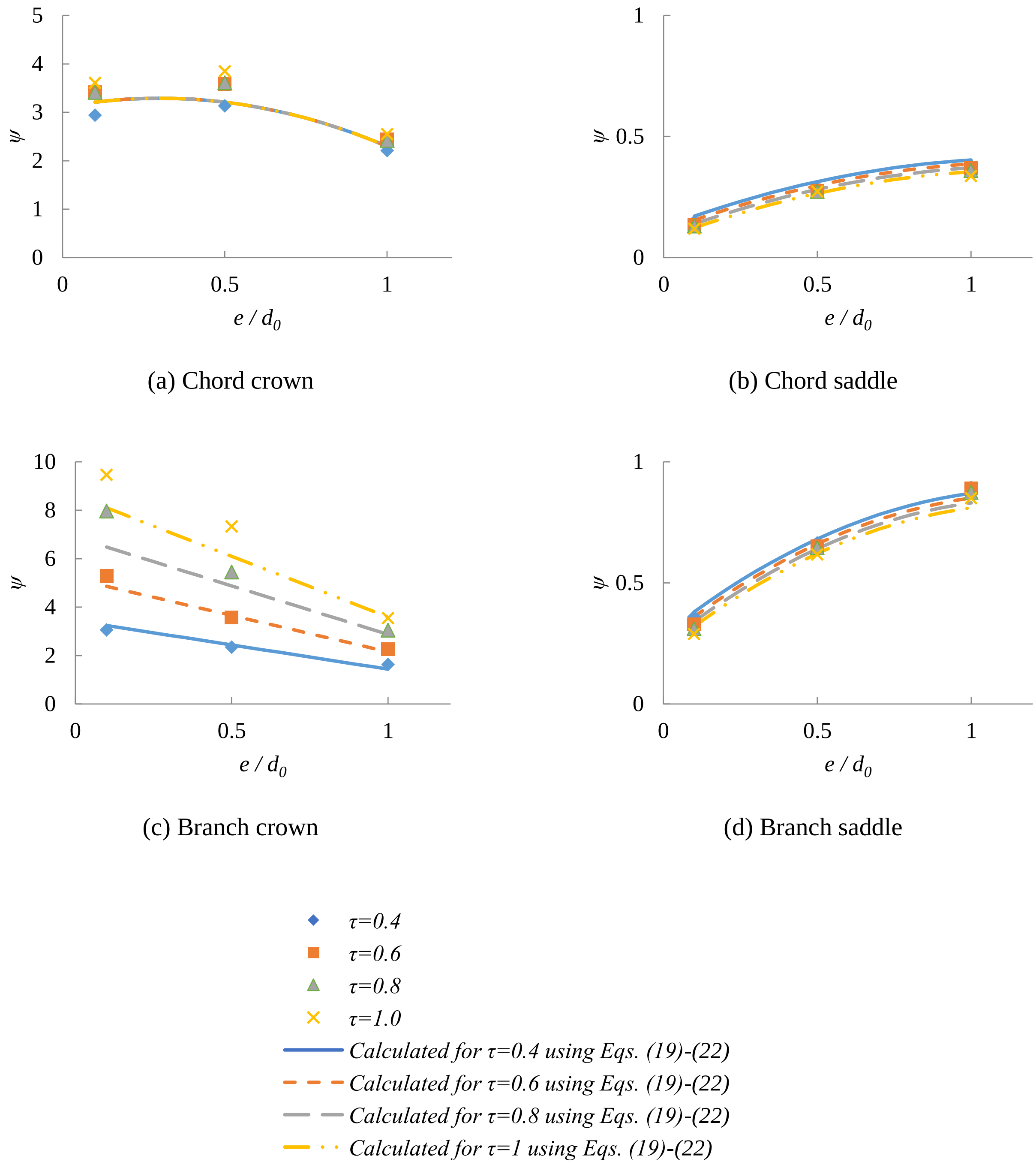

Fig. 15. Effects of e/d_0 and τ on SCFs in connections (β = 0.6 and 2γ = 35)

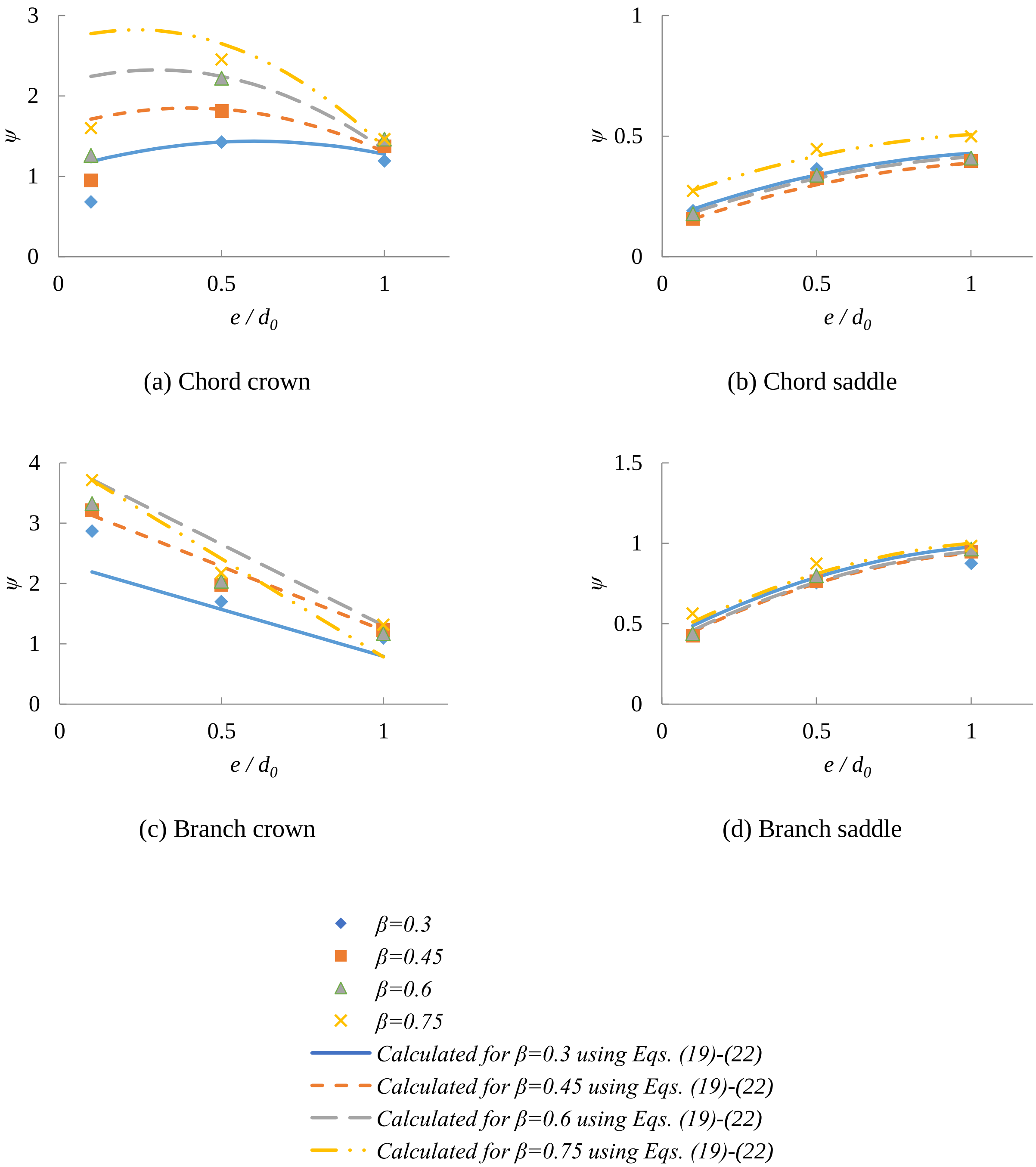

Fig. 16. Effects of e/d_0 and β on SCFs in connections ($2\gamma = 20$ and $\tau = 0.6$)

5.3. Proposed Formulae

The parametric study presented in Section 5.2 showed that the existing SCF formulae in CIDECT DG8 [8] for regular CHS-to-CHS X-connections under branch axial loading, utilizing the F_2 factor [Eq. (17)], produce unsafe predictions when applied to chord-end CHS X-connections with cap plates. Like the approach presented in Section 4.3, this section presents formulae for correction factors (ψ) to consider the effects of chord end distance and cap plate in SCF calculation.

After an extensive evaluation of different types of formulae, and a subsequent non-linear least-squares regression analysis, the approximate "best-fit" equations are given, as follows:

- For the chord saddle:

$$\psi = 0.483 + 0.474(e/d_0) + 1.49(\beta)^2 - 0.081(\tau) - 1.33(\beta) - 0.003(\beta)(2\gamma) - 0.197(e/d_0)^2 \tag{19}$$

- For the chord crown:

$$\psi = 1.22(e/d_0) + 0.219(\beta)(2\gamma) - 0.00203(\beta)(2\gamma)^2 - 3.38(\beta)(e/d_0)^2 \tag{20}$$

- For the branch saddle:

$$\psi = 0.862 + (e/d_0) + (\beta)^2 + 0.0001(2\gamma)^2 - (\beta) - 0.012(2\gamma) - 0.100(\tau) - 0.414(e/d_0)^2 \tag{21}$$

- For the branch crown:

$$\psi = 9(\beta)(\tau) + 0.216(\beta)(2\gamma)(\tau) - 0.035(2\gamma)(\tau)(e/d_0) - 6.30(\beta)(\tau)(e/d_0) - 10.3(\beta)^4(\tau) \tag{22}$$

Figs. 14-16 show sample comparisons between the above equations and the ψ-values obtained by dividing $SCF_{end\ connection}$ by $SCF_{control\ model}$ (based on the parametric study). Table 4 includes the key statistics from the comparison. As shown in Figs. 14-16 and Table 4, Eqs. (19)-(22) are reasonably accurate over the range of parameters considered. For consistency with CIDECT DG8 [8], a minimum SCF-value of 2.0 is still recommended.

Table 4. Mean values and COVs of FE-to-predicted ψ based on 180 CHS-to-CHS cap plate-reinforced end X-connection models

Location	Equation No.	Mean	COV
Chord Saddle	(19)	1.01	0.11
Chord Crown	(20)	0.97	0.18
Branch Saddle	(21)	1.00	0.06
Branch Crown	(22)	1.01	0.23

6. Conclusions

To establish definitive design provisions for chord-end RHS-to-RHS and CHS-to-CHS X-connections with cap plates, a total of 496 FE models were developed and analysed in the parametric study presented in this paper. Based on the results, SCF correction factors (ψ), and parametric formulae to estimate ψ based on chord end distance-to-width (or diameter) (e/b_0 or e/d_0), branch-to-chord width (β), branch-to-chord thickness (τ), and chord slenderness (2γ) ratios, were derived. The ψ formulae developed in this study can be used in conjunction with the existing SCF formulae in CIDECT Design Guide 8 (or other design guides) for calculation of SCFs in cap plate-reinforced RHS-to-RHS and CHS-to-CHS end connections.

Acknowledgements

The authors would like to express their appreciation to the Natural Sciences and Engineering Research Council of Canada (NSERC) for providing the financial support for this research.

Nomenclature

E	Young's modulus
F_2	reduction factor to account for "end effects" in CIDECT Design Guide 8
$L_{r,max}$	distance from weld toe to end point of extrapolation zone
$L_{r,min}$	distance from weld toe to starting point of extrapolation zone
SCF_A	branch SCF at hot spot A
SCF_B	chord SCF at hot spot B
SCF_C	chord SCF at hot spot C
SCF_D	chord SCF at hot spot D
SCF_E	branch SCF at hot spot E
$SCF_{b\_crown,ax}$	branch SCF at the crown point
$SCF_{b\_saddle,ax}$	branch SCF at the saddle point
$SCF_{ch\_crown,ax}$	chord SCF at the crown point
$SCF_{ch\_saddle,ax}$	chord SCF at the saddle point
$SCF_{end\ connection}$	SCF in end-connection model
$SCF_{control\ model}$	SCF in control model (connection with sufficient chord continuity)
$SCF_{end,i}$	SCF at hot spot *i* in an RHS-to-RHS axially loaded X-connection near an open chord end
SCF_i	SCF at hot spot *i* in an RHS-to-RHS axially loaded X-connection
$X_{1\text{-}4}$	SCF parameter for CHS-to-CHS X-connections
b_0	RHS chord width
b_1	RHS branch width
b_p	branch plate width
d_0	CHS chord diameter
d_1	CHS branch diameter
e	end distance = distance from the heel/toe of the closest branch to the chord end
e_{min}	minimum required end distance
h_0	chord height
h_1	branch height
l_0	chord length
r_i	inner corner radius
r_o	outer corner radius
r_1	inner radius of CHS branch member
r_0	outer radius of CHS chord member
t_0	chord wall thickness
t_1	branch wall thickness

α	chord length parameter (= $2l_0/d_0$)
β	branch-to-chord diameter ratio (= d_1/d_0); branch-to-chord width ratio (= b_1/b_0)
γ	half chord diameter-to-thickness ratio (= $d_0/2t_0$); half chord width-to-thickness ratio (= $b_0/2t_0$)
τ	branch-to-chord thickness ratio (= t_1/t_0)
θ	acute angle between the branch and chord (in degrees)
ψ	reduction factor for end connection

References

[1] J.A. Packer, J.E. Henderson, Hollow Structural Section Connections and Trusses – a Design Guide, 2nd ed. Canadian Institute of Steel Construction, Toronto, Canada, 1997.

[2] J. Wardenier, Y. Kurobane, J.A. Packer, A. van der Vegte, X.L. Zhao, Design Guide for Circular Hollow Section (CHS) Joints under Predominantly Static Loading, CIDECT Design Guide No. 1, 2nd ed. CIDECT, Geneva, Switzerland, 2008.

[3] J.A. Packer, J. Wardenier, X.L. Zhao, G.J. van der Vegte, Y. Kurobane, Design Guide for Rectangular Hollow Section (RHS) Joints under Predominantly Static Loading, CIDECT Design Guide No. 3, 2nd ed. CIDECT, Geneva, Switzerland, 2009.

[4] ISO (International Organization for Standardization), ISO 14346:2013, Static Design Procedure for Welded Hollow Section Joints – Recommendations, Geneva, Switzerland, 2013.

[5] AISC (American Institute of Steel Construction), ANSI/AISC 360-16, Specification for Structural Steel Buildings. Chicago, IL, USA, 2016.

[6] J.A. Packer, D.R. Sherman, M. Lecce, Design Guide No. 24, Hollow Structural Section Connections. American Institute of Steel Construction, Chicago, IL, USA, 2010.

[7] CEN (European Committee for Standardization), EN 1993-1-8:2010, Eurocode 3: Design of Steel Structures – Part 1–8: Design of Joints, Brussels, Belgium, 2010.

[8] X.L. Zhao, S. Herion, J.A. Packer, R.S. Puthli, G. Sedlacek, J. Wardenier, K. Weynand, A.M. van Wingerde, N.F. Yeomans, Design Guide for Circular and Rectangular Hollow Section Welded Joints under

Fatigue Loading, CIDECT Design Guide No. 8, CIDECT and Verlag TÜV Rheinland GmbH, Köln, Germany, 2001.

[9] ISO (International Organization for Standardization), ISO 14347:2008, Fatigue – Design Procedure for Welded Hollow-Section Joints – Recommendations, Geneva, Switzerland, 2008.

[10] G.J. van der Vegte, Y. Makino, Further research on chord length and boundary conditions of CHS T- and X-joints. Advanced Steel Construction 6(3) (2010) 879-890.

[11] G.J. van der Vegte, Y. Makino, Ultimate strength formulation for axially loaded CHS uniplanar T-joints, International Journal of Offshore and Polar Engineering (2006) 16(4) 305-312.

[12] A.P. Voth, J.A. Packer, Branch plate-to-circular hollow section connections. II: X-type parametric numerical study and design. Journal of Structural Engineering, American Society of Civil Engineers, 138(8) (2012) 1007–1018.

[13] A.P. Voth, J.A. Packer, Numerical study and design of T-type branch plate-to-circular hollow section connections. Engineering Structures 41 (2012) 477–489.

[14] Y.J. Fan, J.A. Packer, RHS-to-RHS axially loaded X-connections near an open chord end. Canadian Journal of Civil Engineering 44 (2017) 881-892.

[15] X.D. Bu, J.A. Packer. Chord end distance effect on RHS connections. Journal of Constructional Steel Research, 168 (2020) 105992.

[16] K. Tousignant, Effect of chord length and boundary conditions on welds in CHS X-joints. Proceedings of the 17th International Symposium on Tubular Structures, Singapore (2019) 63-70.

[17] CEN (European Committee for Standardization), Eurocode 3: Design of steel structures – Part 1–8: Design of joints. prEN 1993-1-8:2018, Brussels, Belgium, 2018.

[18] S. Daneshvar, M. Sun, K. Tousignant, Stress concentration factors for RHS-to-RHS X-connections near an open chord end. Journal of Constructional Steel Research 175 (2020) 106352.

[19] A. Ziaei Nejad, M. Sun, K. Tousignant, Circular hollow section X-connections near an open chord end: stress concentration factors. Journal of Constructional Steel Research 177 (2020) 106454.

[20] Swanson Analysis Systems, ANSYS ver. 14.0. Houston, TX, USA, 2011.

[21] Dassault Systèmes, ABAQUS ver. 6.14. Providence, RI, USA, 2014.

[22] S. Daneshvar, M. Sun, K. Karimi, Galvanized RHS X-connections. I: effects of vent and drain holes on SCFs. Journal of Constructional Steel Research 167 (2020) 105854.

[23] S. Daneshvar, M. Sun, Stress concentration factors of RHS T-connections with galvanizing holes under in-plane bending. Journal of Constructional Steel Research 169 (2020) 106039.

[24] B. Cheng, Q. Qian, X.L. Zhao, Numerical investigation on stress concentration factors of square bird-beak SHS T-joints subject to axial forces. Thin-Walled Structures 94 (2015) 435-445.

[25] L.W. Tong, G.W. Xu, Y.Q. Liu, D.Q. Yan, X.L. Zhao, Finite element analysis and formulae for stress concentration factors of diamond bird-beak SHS T-joints. Thin-Walled Structures 86 (2015) 108-120.

[26] L.W. Tong, G.W. Xu, D.L. Yang, F.R. Mashiri, X.L. Zhao, Stress concentration factors in CHS-CFSHS T-joints: experiments, FE analysis and formulae. Engineering Structures 151 (2017) 406-421.

[27] R. Feng, B. Young, Stress concentration factors of cold-formed stainless steel tubular X-joints. Journal of Constructional Steel Research 91 (2013) 26-41.

[28] K. Tousignant, J.A. Packer, Fillet weld effective lengths in CHS X-connections. I: Experimentation. Journal of Constructional Steel Research 128 (2017) 420-431.

[29] K. Tousignant, J.A. Packer, Numerical investigation of fillet welds in HSS-to-rigid end-plate connections. Journal of Structural Engineering, ASCE 143(12) (2017) 04017165:1-04017165-16.

[30] K. Tousignant, J.A. Packer, Fillet weld effective lengths in CHS X-connections. II: Finite element modelling, parametric study and design. Journal of Constructional Steel Research 141 (2018) 77-90.

[31] K. Tousignant, J.A. Packer, Weld effective lengths for round HSS cross-connections under branch axial loading. Engineering Journal, AISC 56(3) (2019) 173-186.

[32] K. Tousignant, J.A. Packer, Fillet welds around circular hollow sections. Welding in the World, IIW 63 (2019) 421-433.

[33] H. Ahmadi, A. Ziaei Nejad, Local joint flexibility of two-planar tubular DK-joints in OWTs subjected to axial loading: parametric study of geometrical effects and design formulation. Ocean Engineering 136(5) (2017) 1-10.

[34] H. Ahmadi, A. Ziaei Nejad, A study on the local joint flexibility (LJF) of two-planar tubular DK-joints in jacket structures under in-plane bending loads. Applied Ocean Research 64(3) (2017) 1-14.

[35] H. Ahmadi, A. Ziaei Nejad, (2017). Geometrical effects on the local joint flexibility of two-planar tubular DK-joints in jacket substructure of offshore wind turbines under OPB loading. Thin-Walled Structures 114(5) (2017) 122-133.

[36] H. Ahmadi, A. Ziaei Nejad, Stress concentration factors in uniplanar tubular KT-joints of jacket structures subjected to in-plane bending loads. International Journal of Maritime Technology 5(2) (2016) 27-39.